Studies of Functionalized Poly(phenylenevinylene)s

Wai-Kin Chan and Luping Yu*

Department of Chemistry, The University of Chicago, 5735 South Ellis Avenue, Chicago, Illinois 60637

Received May 10, 1995; Revised Manuscript Received July 10, 1995[⊗]

ABSTRACT: This paper reports the synthesis of poly(phenylenevinylene) functionalized with a push−pull nonlinear optical (NLO) chromophore. The initial aim to synthesize these polymers was to study their photorefractive effect. In contrast to our expectation, the polymers did not show any photorefractive phenomenon although they did exhibit two necessary properties for the photorefractive effect: photoconductivity and electro-optical activity. Detailed physical property studies have been carried out on these polymers, including measurements of photoconductivity, second harmonic generation, and electro-optic coefficients. An interesting liquid crystallinity was also observed in these polymers.

Introduction

It is known that the photorefractive (PR) effect can be utilized in many optical devices, such as information storage, dynamic holography, and phase conjugator.[1] Photorefractive phenomena have been studied for almost 30 years, mainly focusing upon inorganic materials, such as ferroelectric single crystals ($LiNbO_3$, $BaTiO_3$).[1] Recently, photorefractive polymers have emerged as a new kind of optical material.[2] It is expected that these materials possess unique properties supplemental to their inorganic counterparts, such as ease of preparation for large area samples, low dielectric constant, high optical performance, and low cost. By their nature, photorefractive polymers are multifunctional polymers which combine photoconductivity and electro-optical activity together to manifest photorefractivity. In the past several years, two approaches have been developed to synthesize or prepare photorefractive polymeric materials, namely, the composite material approach and fully functionalized polymer approach.[2−5] Both approaches have enjoyed successes in identifying photorefractive polymers.

Our research group has been mainly involved in synthesizing fully functionalized PR polymers. Three polymer systems have been developed; functionalized polyurethanes,[3] functionalized conjugated polymers,[4] and polyimides[5] containing porphyrin and NLO chromophore units. It was found that the conjugated polymers are very interesting systems due to their richness in structural variations. Our first conjugated photorefractive polymer contains a poly(phenylene-*co*-thiophene) backbone.[3] An obvious extension is to utilize other conjugated polymer backbones. The poly(phenylenevinylene) (PPV) backbone is one of the choices because it exhibits high photoconductivity.[6] It is also known that PPV backbones are easy to be functionalized by utilizing the Heck coupling reaction.[7] In this paper we report the synthesis of a series of functionalized PPV copolymers. Two dibromobenzene derivatives substituted with a NLO chromophore and an alkoxy group were used as monomers. These monomers were copolymerized with *p*-divinylbenzene to give the resulting copolymers. However, detailed photorefractive studies revealed that although the copolymers possessed both photoconductivity and electro-optic activity, the polymer systems exhibited no photorefractive phenomenon. This is one example which shows the complication in designing PR polymers; the existence of two necessary physical properties in a single polymer does not sufficiently ensure the polymer to be photorefractive. Fortunately, other physical properties of these polymers are interesting enough to disclose the experimental results. It was found that several polymers are liquid crystalline materials. The interesting results was that even though the monomer bearing the nonlinear optical (NLO) chromophore (amino(methylsulfonyl)stilbene) did not show LC properties, several polymers obtained still exhibited nematic LC properties. This paper reports these results.

Experimental Section

Tetrahydrofuran (THF) was distilled over sodium benzophenone ketyl. All other chemicals were purchased from Aldrich Chemical Co. and used as received unless otherwise stated. *p*-Divinylbenzene[8] and 2,5-dibromophenol[9] were synthesized according to the literature procedure.

General Procedure for Synthesizing 2,5-Dibromoalkoxybenzenes. 2,5-Dibromophenol (4.55 g, 18.1 mmol), alkyl bromide (18.1 mmol), potassium carbonate (2.5 g, 18.1 mmol), and acetone (50 mL) were added to a 100 mL two-necked, round-bottomed flask under a nitrogen atmosphere. The resulting mixture was refluxed for 24 h, and water (50 mL) was then added. The mixture was extracted with ether (3 × 50 mL). The combined organic layer was dried over anhydrous magnesium sulfate and then concentrated. The crude product was separated by silica gel chromatography using hexane as eluent.

2,5-Dibromo-1-hexoxybenzene (2a): yield 89%; ^{1}H NMR ($CDCl_3$, ppm) δ 7.32 (d, J = 8.4 Hz, 1 H), 6.95 (d, J = 1.1 Hz, 1 H), 6.90 (dd, J = 1.1, 8.4 Hz, 1 H), 3.97 (t, J = 6.4 Hz, 2 H), 1.82 (m, 2 H), 1.49 (m, 2 H), 1.35 (m, 4 H), 0.91 (t, J = 6.6 Hz, 3 H); ^{13}C NMR ($CDCl_3$) δ 156.3, 134.2, 124.6, 121.6, 116.6, 111.2, 69.6, 31.6, 29.1, 25.8, 22.8, 14.2; FTIR (neat) 2954, 2931, 2871, 2858, 1577, 1558, 1478, 1466, 1398, 1386, 1261, 1251, 1129, 1082, 1034, 1016, 994, 873, 837, 798 cm^{-1}. Anal. Calcd for $C_{12}H_{16}Br_2O$: C, 42.89; H, 4.80. Found: C, 42.94; H, 4.77.

2,5-Dibromo-1-dodecoxybenzene (2b): yield 78%; mp 31−32 °C; ^{1}H NMR ($CDCl_3$, ppm) δ 7.32 (d, J = 8.2 Hz, 1 H), 6.94 (d, J = 1.5 Hz, 1 H), 6.90 (dd, J = 1.5, 8.2 Hz, 1 H), 3.97 (t, J = 6.4 Hz, 2 H), 1.82 (m, 2 H), 1.48 (m, 2 H), 1.25−1.35 (m, 16 H), 0.88 (t, J = 6.2 Hz, 3 H); ^{13}C NMR ($CDCl_3$) δ 156.3, 134.2, 124.6, 121.6, 116.5, 111.2, 69.6, 32.1, 29.9, 29.8, 29.6, 29.5, 29.1, 26.1, 22.9, 14.3; FTIR (neat) 2956, 2920, 2870, 2851, 1578, 1558, 1478, 1467, 1399, 1387, 1284, 1261, 1250, 1128, 1082, 1035, 1024, 1005, 870, 827, 801 cm^{-1}. Anal. Calcd for $C_{18}H_{28}Br_2O$: C, 51.45; H, 6.72. Found: C, 51.57; H, 6.80.

2,5-Dibromo-1-(1-pentylhexoxy)benzene (2c): 6-Undecanol (2.3 g, 13.1 mmol), 2.5-dibromophenol (3.0 g, 11.9 mmol), triphenylphosphine (4.7 g, 17.9 mmol), and THF (30

[⊗] Abstract published in *Advance ACS Abstracts,* September 1, 1995.

0024-9297/95/2228-6410$09.00/0

mL) were added to a 100 mL two-necked round-bottomed flask under a nitrogen atmosphere. The solution was cooled to 0 °C, and diethyl azodicarboxylate (DEAD) (2.3 mL, 14.3 mmol) was then added dropwise to the reaction mixture. The solution was stirred for 5 h at room temperature. After the solvent was removed with a rotary evaporator, the crude product was separated by silica gel chromatography using hexane as the eluent. The product was collected as a colorless liquid (4.8 g, 99% yield): ^{1}H NMR (CDCl$_3$, ppm) δ 7.31 (d, J = 8.4 Hz, 1 H), 6.92 (d, J = 1.6 Hz, 1 H), 6.87 (dd, J = 1.6, 8.4 Hz, 1 H), 4.21 (quin, J = 5.8 Hz, 1 H), 1.71–1.60 (m, 4 H), 1.45–1.26 (m, 12 H), 0.88 (t, J = 6.8 Hz, 6 H); ^{13}C NMR (CDCl$_3$) δ 156.0, 134.4, 124.5, 121.5, 118.0, 112.3, 80.4, 33.7, 32.0, 25.0, 22.8, 14.2; FTIR (neat) 2955, 2932, 2871, 2859, 1575, 1556, 1467, 1394, 1379, 1249, 1130, 1081, 1033, 997, 951, 877, 839, 796 cm^{-1}. Anal. Calcd for $C_{17}H_{26}Br_2O$: C, 50.27; H, 6.45. Found: C, 50.41; H, 6.41.

Compound 2d. 4′-[(6-Hydroxyhexyl)methylamino]-4-(methylsulfonyl)-stilbene[10] (7.7 g, 19.8 mmol), 2,5-dibromophenol (5.0 g, 19.8 mmol), triphenylphosphine (7.8 g, 29.7 mmol), and THF (60 mL) were added to a 100 mL two-necked round-bottomed flask under a nitrogen atmosphere. The solution was cooled to 0 °C, and diethyl azodicarboxylate (3.1 mL, 19.8 mmol) was added dropwise to the reaction mixture. the solution was stirred for 18 h at room temperature. After the solvent was removed with a rotary evaporator, the crude product was separated by a silica gel chromatography column using methylene chloride as the eluent. The product collected was then recrystallized with a chloroform/methanol mixture. The product collected was yellow crystalline solid (9.5 g, 77% yield): mp 108–109 °C; ^{1}H NMR (CDCl$_3$, ppm) δ 7.81 (d, J = 8.2 Hz, 2 H), 7.55 (d, J = 8.2 Hz, 2 H), 7.36 (d, J = 8.5 Hz, 2 H), 7.33 (d, J = 8.3 Hz, 1 H), 7.13 (d, J = 16.2 Hz, 1 H), 6.95 (d, J = 1.2 Hz, 1 H), 6.91 (dd, J = 1.2, 8.3 Hz, 1 H), 6.85 (d, J = 16.2 Hz, 1 H), 6.63 (d, J = 8.5 Hz, 2 H), 3.97 (t, J = 6.2 Hz, 2 H), 3.36 (t, J = 7.2 Hz, 2 H), 3.03 (s, 3 H), 2.97 (s, 3 H), 1.84 (m, 2 H), 1.64 (m, 2 H), 1.55 (m, 2 H), 1.42 (m, 2 H); FTIR (KBr) 2935, 2855, 1606, 1586, 1521, 1478, 1467, 1385, 1297, 1140, 1088, 1033, 965, 954, 869, 826, 802, 771 cm^{-1}. Anal. Calcd for $C_{28}H_{31}Br_2NO_3$: C, 54.12; H, 5.03; N, 2.25. Found: C, 54.50; H, 4.77; N, 2.38.

Polymerization. A typical procedure for the synthesis of polymer **H** is described as follows: *p*-Divinylbenzene (0.132 g, 1.014 mmol), compound **2c** (0.412 g, 1.014 mmol), palladium(II) acetate (9.1 mg, 4 mol %), tris(*o*-methylphenyl)phosphine (62 mg, 0.2 equiv), and DMF (5 mL) were added into a two-necked round-bottom flask under a nitrogen atmosphere. After a homogeneous solution was obtained, tributylamine (0.7 mL, 3 equiv) was added to the solution. The reaction mixture was stirred at 100 °C for 24 h and then poured into an excess amount of methanol (100 mL). The polymer was collected by filtration; it was redissolved in TCE and precipitated again into methanol. The collected orange-yellow solid was washed in a Soxhlet extractor with methanol for 2 days, and the final yield of the polymer was 71%.

Polymer Characterization. The ^{1}H NMR spectra were collected on a UC 500 MHz spectrometer. The ^{13}C spectra were obtained using a GE QE 300-MHz spectrometer. The FTIR spectra were recorded on a Nicolet 20 SXB FTIR spectrometer. The UV–vis spectra were recorded on a Perkin-Elmer Lambda 6 UV/vis spectrophotometer. GPC measurements were performed using a Waters RI system equipped with a UV detector, a differential refractometer detector, and an Ultrastyragel linear column at 35 °C using THF as the eluent. The molecular weights were calculated on the basis of monodispersed polystyrene standards. Thermal analyses were performed by using DSC-10 and TGA-50 systems from TA instruments under a nitrogen atmosphere with heating rates of 10 and 15 °C/min, respectively. The polarizing microscopic observation was performed with a Nikon OPTIPHOT-2 microscope equipped with a Creative Devices 50-600 high-temperature stage.

The photoconductivity was studied by measuring the voltage resulting from a photocurrent running through the sample and across a 1 MΩ resistor.[11] A He–Ne laser (632.8 nm) was used as the light source.

Scheme 1. Synthesis of Monomers

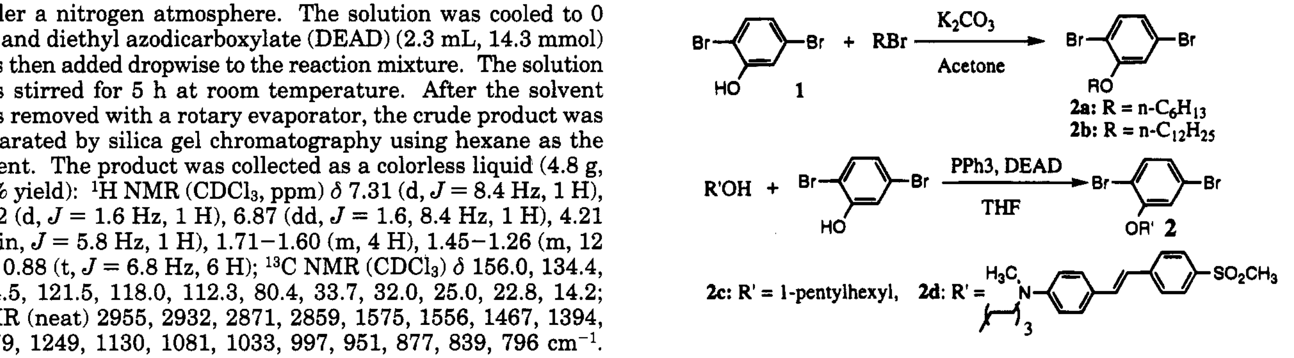

Scheme 2. Polymerization Utilizing the Heck Coupling Reaction

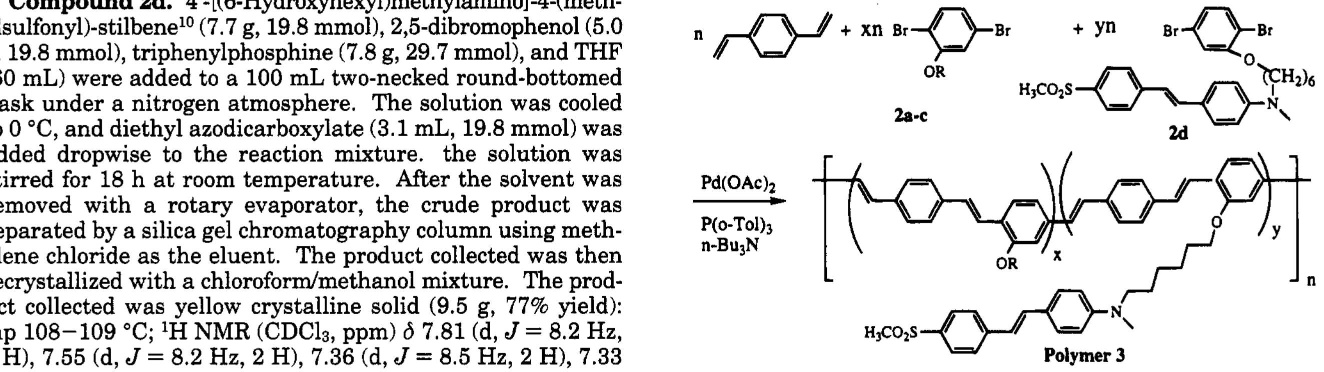

The second-order NLO activities of corona-poled polymer films were characterized by performing a second harmonic generation experiment. The poling conditions were as follows: temperature, 100 °C; voltage, 3 kV at the needle point; gap distance, 1 cm; poling current, <1 μA. A mode-locked Nd:YAG laser (Continuum PY61C-10, 10 Hz repetition rate) was used as the light source. The second harmonic signal generated by the fundamental wave (1064 nm) was detected by a photomultiplier tube (PMT). After amplification it was averaged in a boxcar integrator. A quartz crystal was used as the reference sample.

An electro-optic coefficient (r_{33}) was determined by the simple reflection technique.[12] A polymer film with a thickness of 2–3 μm was prepared by casting a TCE solution of polymer onto an indium–tin oxide (ITO) glass. After corona poling, a silver electrode of 700 Å was deposited on the polymer film by vacuum evaporation. A He–Ne laser (632.8 nm) and a diode laser (780 nm) were used as the light sources.

Cyclic voltammetry (CV) was performed in an EG&G Princeton Applied Research potentiostat interfaced to a personal computer. A thin polymer film was coated onto a Pt disk working electrode (diameter = 2 mm). The counter and reference electrodes were both Pt wire, and the system was calibrated against the formal potential of the [Cp$_2$Fe]/[Cp$_2$Fe$^+$] couple (+0.40 V vs SCE). The experiment was carried out in acetonitrile (10 mL) with tetrabutylammonium tetrafluoroborate (0.33 g) as a supporting electrolyte under a nitrogen atmosphere.

Results and Discussion

Monomer Synthesis and Polymerization. The monomer **2d** was easily synthesized from 2,5-dibromophenol and a NLO chromophore bearing hydroxyl groups by utilizing the Mitsunobu reaction (Scheme 1).[13] Polymerizations were carried out according to Scheme 2. A typical heck reaction condition was applied as described previously:[6] DMF was used as the solvent; the catalyst system was composed of Pd(OAc)$_2$ (4 mol %), tributylamine and triarylphosphine. By changing the ratio of the initial monomer additions, we prepared

Table 1. Synthetic and Phase Transition Data for PPVs[a]

polymer	x	y	R	solubility	yield (%)	T_g (°C)	T_m (°C)	T_i (°C)	T_d (°C)
A	0	1		N	81	110	160[b]		399
B	1	0	*n*-hexyl	N	94		239	260[c]	420
C	0.5	0.5	*n*-hexyl	N	88	113	*d*	*d*	410
D	0.1	0.9	*n*-hexyl	N	68	112	*d*	*d*	399
E	1	0	*n*-dodecyl	TCE[e]	82	113	140[f]	200[c]	418
F	0.5	0.5	*n*-dodecyl	N	81	98	*d*	*d*	396
G	0.1	0.9	*n*-dodecyl	N	88	115	*d*	*d*	393
H	1	0	1-petnylhexyl	TCE, $CHCl_3$	71	125	160	202[c]	360
I	0.7	0.3	1-pentylhexyl	TCE	82	90	130[f]	210[c]	370
J	0.5	0.5	1-pentylhexyl	TCE, DMF	73	92	150[f]	200[c]	342
K	0.1	0.9	1-pentylhexyl	N	89	105	180[b]		387

[a] N = insoluble in common organic solvents; T_g = glass transition temperature; T_m = melting temperature; T_i = isotropization temperature; T_d = decomposition temperature determined by the onset of weight loss from TGA thermograms. [b] Polymer melt was very viscous, no liquid crystalline phase was observed until cross-linking started. [c] This is the temperature at which cross-linking started; the liquid crystalline texture disappeared gradually under polarized microscope. [d] No phase transition could be observed; the polymer was infusible solid. [e] Soluble only in low concentrations. [f] No obvious transition could be observed from DSC; this temperature was obtained from polarized microscopy.

polymer with different compositions (varying x/y ratio) (Table 1). By changing the composition, the processability of the resulting polymers can be improved and their physical properties can be varied. It was observed that those polymers which were insoluble in organic solvents formed gels after 3–5 h of reaction.

It was also found that the solubilities of these polymers depend upon two major factors: the size of the alkyl chain and the concentration of the chromophore attached. The first polymer synthesized was polymer **A** bearing a NLO chromophore which was insoluble in most of the common organic solvents, such as THF, TCE, DMF, etc. The reason is not very clear, and a possible explanation is due to the high chromophore concentration which brings a strong intermolecular interaction. In order to enhance the solubility, we attempted to use other dibromoalkoxybenzenes as comonomers to reduce the chromophore concentration. Copolymers resulting from the addition of comonomer **2a** (R = hexyl group) were still insoluble (polymers **B**, **C**, and **D**). When R was the dodecyl group, only polymer **E**, which bears no NLO chromophore, was soluble. Polymers **F** and **G**, which contain 50% and 90% NLO chromophore, respectively, were still insoluble. However, when a secondary 1-pentylhexyl group was introduced as the side chain, the solubilities of the resulting copolymers were enhanced if the chromophore concentration was low to medium. For example, polymers **H**, **I**, and **J** were all soluble in tetrachloroethane (TCE). The reason for the enhancement in solubility can be attributed to the steric hindrance of the secondary alkoxy group which effectively reduces the intermolecular interaction between polymer chains. If the chromophore concentration was high (polymer **K**, 90% chromophore), the polymer became insoluble again.

Structural Characterization. From the ^1H NMR spectra of soluble polymers **H** and **I**, the detailed analysis of these spectra is difficult to do due to the overlapping and broadening of peaks, but the spectral features are consistent with the polymer structures. The chemical shifts at 7.9, 7.6, 7.3, and 6.7 ppm for polymer **I** correspond to the aromatic protons on the stilbene, and this indicates the presence of a NLO chromophore in polymer **I**. The ratio of the integration of chemical shifts of the methyl group on the sulfonyl and the alkoxy group for polymer **I** is consistent with the monomers ratio. The spectral features of the soluble polymers **E** and **J** are similar to those of polymers **H** and **I**, respectively.

In the FTIR spectra of polymers **H** and **I**, the absorption band at 822 cm^{-1} is ascribed to the out-of-plane bending of the C–H bond in a 1,4-disubstituted benzene. Another strong absorption band was observed at 957 cm^{-1}, which is a typical absorption of the out-of-plant bending vibration of the trans-substituted vinylene group. The polymers with a NLO chromophore exhibit a strong SO_2 stretching band at 1145 cm^{-1} due to the presence of the NLO chromophore in addition to the spectral features similar to polymer **H**.

The UV/vis spectra of the soluble polymers showed red shifts of 20 nm in the absorption peaks (around 422 nm) compared with the unsubstituted PPV (400 nm). For polymers **H** and **I**, the absorption bands of the chromophore and the conjugated backbone overlapped and could not be distinguished. All of the insoluble polymers were yellow solids and their electronic transitions were not studied.

Thermal and Liquid Crystalline Properties of PPV. The data of thermal properties of polymers are summarized in Table 1. TGA thermograms showed that all of the polymers were stable up to 350 °C under a nitrogen atmosphere. DSC studies showed that polymers without the attached chromophore (polymers **D** and **E**) or with a high chromophore concentration (**A**, **D**, **G**, and **K**) showed a similar glass transition temperature (see Table 1). Polymers **C**, **F**, and **K** possess the same alkoxy/chromophore ratio (1/1), their T_g values change according to the size of the alkoxy groups: polymer **C** (hexyl), 113 °C, polymers **F** (*n*-dodecoxy) 98 °C, and polymer **K** (1-pentylhexoxy), 92 °C, respectively. Typical DSC thermograms of these soluble polymers without chromophore (**E** and **H**) and with chromophore (**I** and **J**) were shown in Figure 1. Besides the glass transition, the traces of the DSC thermograms of these polymers exhibit an exothermic process at ca. 200 °C. This process is clearly due to the cross-linking reaction of the polymer backbone since it can be observed in all of these polymers and no weight loss was observed in TGA studies in that temperature range (170–230 °C). A similar cross-linking process was also observed in our previous dialkoxy-substituted PPVs.[7d]

Under a polarized microscope, the liquid crystalline phase can be observed in polymers **B**, **E**, and **H**–**J** when they are heated on a heating stage. Typical polarized micrographs of polymers **H** and **I** are shown in Figure 2 where a special nematic-phase pattern can be observed with a disclination point of 1. However, the melting temperature of these polymers could not be observed from DSC studies. The melting points reported here were obtained under a microscope, except for polymer **H** which showed a clear melting peak at 160 °C (Figure 1). The formation of a LC phase is due

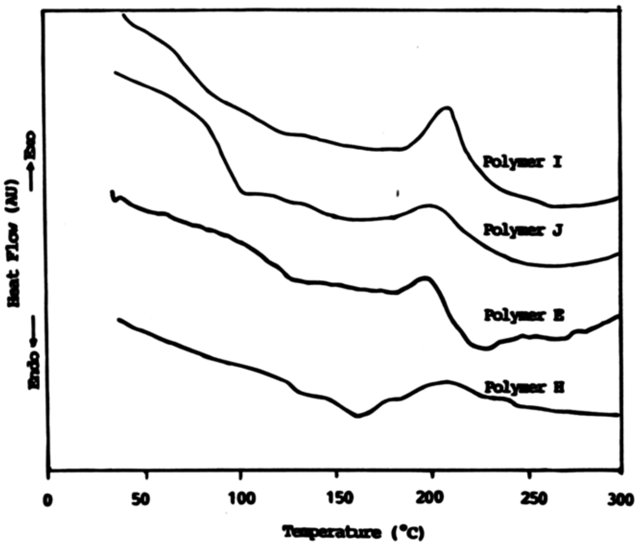

Figure 1. DSC thermograms of polymers **E**, **H**, **I**, and **J**.

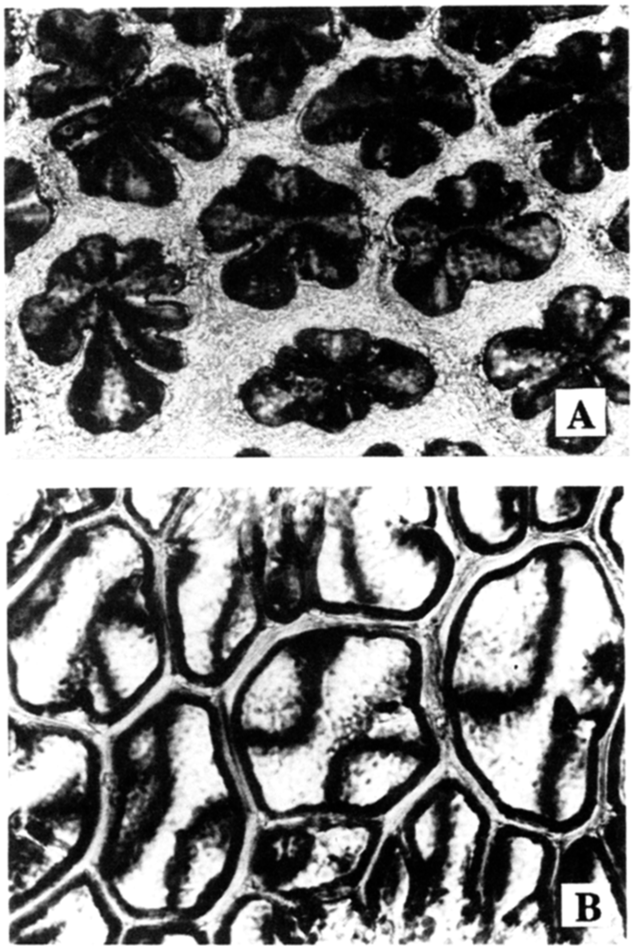

Figure 2. Polarized micrograph of (A) polymer **H** at 160 °C and (B) polymer **I** at 130 °C. The magnification is 276 times.

to the presence of a rigid PPV backbone, because the NLO chromophore does not show any LC behavior.[7d] If the polymers were further heated, they underwent a cross-linking reaction and the polymer melt became immobile and hardened. As a result, the transition from the LC phase to the isotropic phase could not be observed in all of these LC polymer because the LC phase was frozen by cross-linking.

Polymers **C**, **D**, **F**, **G**, and **K** only show glass transitions until cross-linking occurred (ca. 210 °C). It was

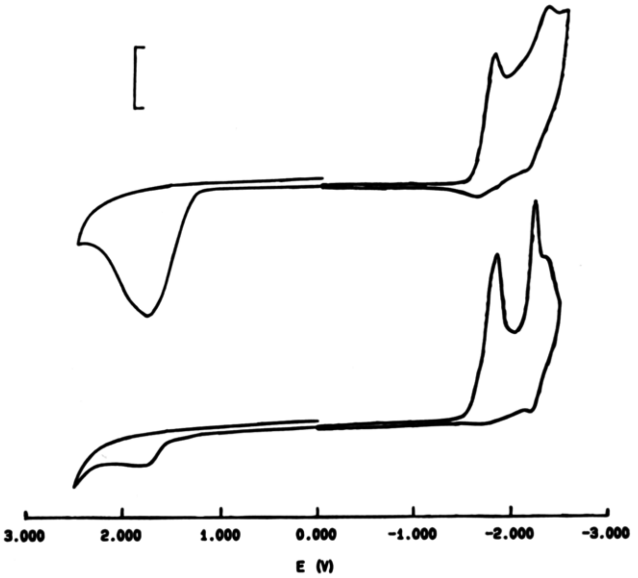

Figure 3. Cyclic voltammograms of polymers **H** and **I** in CH_3CN. n-Bu_4NBF_4 was used as the supporting electrolyte, and the scan rate was 100 mV/s.

mentioned before that these polymers were insoluble. When they were heated on a heating stage, they were found to be infusible although they became soft. Although birefringent patterns were observed in these polymers under a polarized microscope, we do not know whether they are due to the crystallinities of the pristine polymers or the liquid crystalline properties of the polymer melt.

Physical Properties. From the result of the electrochemical studies, one can obtain the information about the redox behavior of the polymer. The cyclic voltammograms of polymers **H** and **I** are shown in Figure 3. Both polymers showed two cathodic waves at −1.87 and −2.27 V, which correspond to the reduction of the polymer backbone. The reverse processes were not very clear. An anodic wave was also observed at 1.75 V due to the oxidation of the polymer. However, no reversible process could be observed and the sample became non-electro-active after successive scans. A possible reason for the irreversibility is that other chemical reactions, instead of charge recombination, occurred after the formation of charge species by the injection/ejection of electrons.

In order to manifest the photorefractivity, the necessary condition is that the polymer must be both photoconductive and electro-optically active. When the He–Ne laser ($\lambda = 632.8$ nm) was irradiated to the polymer thin film sandwiched between ITO and gold electrodes, photocurrents were detected. Figure 4 shows the photocurrents of polymers **H**, **I**, and **J** as a function of the external field. It can be seen that the photocurrents exhibited a strong electric field dependence; as the external field was increased, the photocurrent response increased. The photoconductivities of polymers **H**, **I**, and **J**, deduced from the photocurrent results, were shown in Table 2. From the photocurrent results, the quantum yield of photogeneration of charge carriers can also be deduced (see the inset of Figure 4). The maximum quantum yield was of the order of 10^{-5} at a very high electric fields. Such a low quantum yield may be attributed to a low sensitivity at the working laser wavelength. Similar results were observed for different polymers and the incorporation of a NLO chromophore seems to have little effect on the photoconductivity. The reason for this observation is not clear.

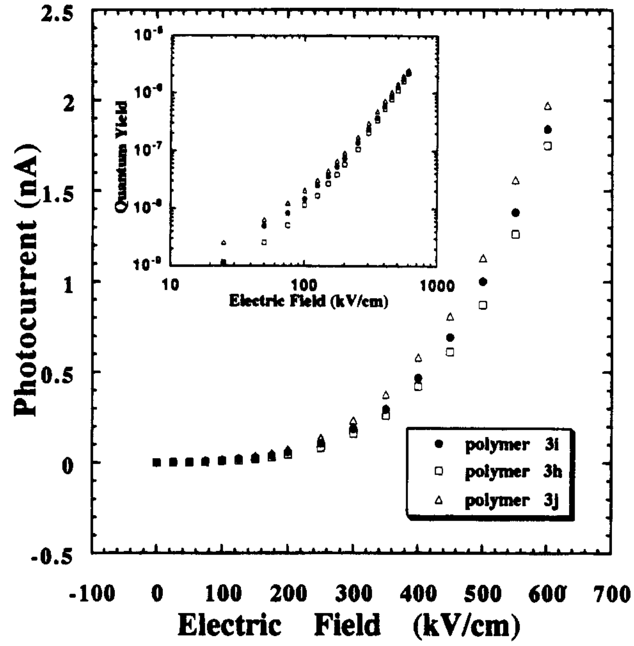

Figure 4. Photocurrent response and quantum yield of charge generation (the inset figure) of polymers **H**, **I**, and **J** as a function of external electric field.

Table 2. Physical Properties of Some Soluble PPVs

poly-mer	$10^{-3}M_n$	PD[a]	λ_{max} (nm)[b]	d_{33}[c] (pm/V)	r_{33} (pm/V) 633 nm	r_{33} (pm/V) 780 nm	photoconductivity[d] ($10^{-11}\ \Omega^{-1}\ cm^{-1}$)
E	3.1[e]	1.46	443				*f*
H	5.4	2.32	440				4.58
I	5.0	3.23	425	18	0.7	0.5	4.82
J	5.0	1.92	420	22	1.9	1.7	5.16

[a] Polydispersity. [b] In tetrachloroethane solution. [c] At 1064 nm. [d] At an electric field of 600 kV/cm. [e] The polymer is not completely soluble in THF; only the soluble part was measured. [f] The polymer solution was too dilute; polymer film could not be prepared.

To study the NLO effect, a poled polymer film was prepared from polymer **I** or **J** by heating up the film in the presence of high voltage in a corona discharge apparatus. The second harmonic coefficient, d_{33} (532 nm), of polymers **I** and **J** were found to be 18 and 22 pm/V, respectively. These values correlate well with the chromophore concentration in the polymers; polymer **J** has a higher density and hence a higher d_{33} value. The thermal stability of the d_{33} value of polymer **I** is shown in Figure 5. These data were obtained by monitoring the second harmonic signal of the poled polymer films when they were heated up in situ. The signal started to decay at ca. 60 °C and dropped to less than 20% at 80 °C. Similar results were obtained by repoling the same sample, indicating that the low stability was primarily due to a low glass transition temperature of the polymer (90 °C), but not due to decomposition of the chromophore. However, if the polymer film was poled at 200 °C for 2 h, the d_{33} value remained identical to the previous results and became more stable; the decay was slowed (20% loss occurred at 100 °C). This result suggests that the cross-linking among the PPV backbone occurred at high temperatures. The network formed helps to stabilize the dipole orientation. Similar results were also obtained for polymer **J**.

Due to the relaxation of the dipole orientation during the process of the silver electrode deposition, the polymer film poled at 100 °C could not be used to study the electro-optic effect. If the film was poled at 200 °C for 2 h, no decay of the second harmonic signal was observed after the silver electrodes were deposited on the film. The electro-optic coefficients, r_{33}, of polymers **I** and **J** at 632.8 and 780 nm are summarized in Table 2. The r_{33} value of polymer **J** is higher than that of **I**, because it has a higher NLO chromophore concentration, like the case of the d_{33} value measurement. Moreover, for the same polymer, the E-O coefficient at 633 nm is larger than that at 780 nm due to a larger resonance enhancement at the wavelength closer to the absorption maximum.

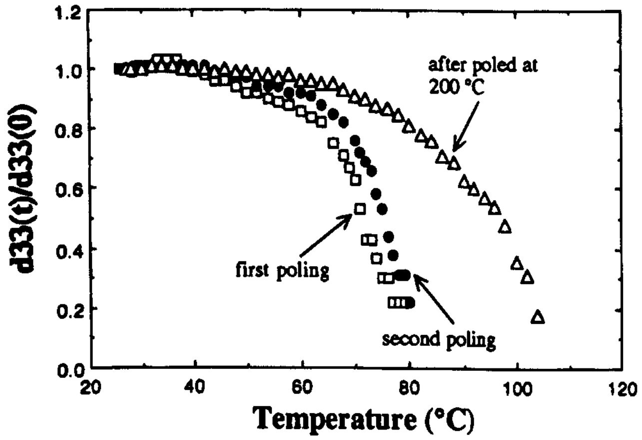

Figure 5. Stability of the second harmonic signal of polymer **I** as a function of temperature.

Since polymers **I** and **J** are both photoconductive and second-order nonlinear optically active, they are expected to be photorefractive. A two beam coupling experiment was performed using a He–Ne laser (632.8 nm) and showed no observable photorefractivity, as indicated by the absence of an asymmetric optical energy exchange which is evidence of the photorefractive effect. The same results were obtained even when the sample was subjected to a high external electric field (600 kV/cm), which is believed to be able to enhance the PR signal. These results demonstrate the complications in designing PR materials. Several factors may contribute to the absence of the PR effect: low quantum yield of photogeneration of charge carriers, low charge carrier mobility, absence of proper charge trapping sites, fast charge recombination, and so on. Much more detailed studies are required to solve the problem.

Conclusion

The Heck reaction has been applied to synthesize PPV functionalized with a push–pull NLO chromophore. The initial aim to synthesize these materials was to study their photorefractive effect. Although the experimental results showed that these polymers exhibit two necessary properties for the photorefractive effect, photoconductivity and electro-optical activity, two beam coupling experiments did not provide positive evidence for the photorefractive effect. However, these polymers showed some interesting properties, such as liquid crystallinity, photoconductivity, optical nonlinearity, and thermal cross-linking. These physical properties together with the chemistry led us to publish this work. An intriguing question is why these polymers are not photorefractive, which can only be answered after a thorough physical study.

Acknowledgment. This work was supported by the Air Force Office of Scientific Research (Grant No. F49620-93-1-0195) and by the National Science Foundation (DMR-9308124). Support from the National Science Foundation Young Investigator program and the Arnold and Mabel Beckman Foundation (Beckman Young Investigator Award) is gratefully acknowledged.

References and Notes

(1) (a) Gunter, P., Huignard, J. P., Eds. *Photorefractive Materials and Their Applications*; Springer-Verlag: Berlin, 1988; Vols. 1, 2. (b) Yariv, A. *Optical Electronics*, 4th ed.; Harcourt Brace Jovanovich: Orlando, FL, 1991.

(2) For a recent review: Moerner, W. E.; Silence, S. M. *Chem. Rev.* **1994**, *94*, 127.

(3) (a) Yu, L.; Chan, W. K.; Bao, Z.; Cao, S. X. F. *J. Chem. Soc., Chem. Commun.* **1992**, 1735. (b) Yu, L.; Chan, W. K.; Bao, Z.; Cao, S. X. F. *Macromolecules* **1993**, *26*, 2216. (c) Chen, Y. M.; Peng, Z. H.; Chan, W, K.; Yu, L. P. *Appl. Phys. Lett.* **1994**, *64*, 1195.

(4) (a) Chan, W. K.; Chen, Y.; Peng, Z.; Yu, L. *J. Am. Chem. Soc.* **1993**, *115*, 11735. (b) Yu, L.; Chen, Y.; Chan, W. K.; Peng, Z. *Appl. Phys. Lett.* **1994**, *64*, 2489. (c) Yu. L.; Chen, Y. M.; Chan, W. K. *J. Phys. Chem.* **1995**, *99*, 2797.

(5) Pent, Z.; Bao, Z.; Yu, L. *J. Am. Chem. Soc.* **1994**, *116*, 6003.

(6) (a) *Handbook of Conducting Polymers*; Skotheim, T. A., Ed.; Marcel Dekker Inc.: Basel, 1989. (b) *Electroresponsive Molecular and Polymeric Systems*; Skotheim, T. A., Ed.; Marcel Dekker Inc.: Basel, 1991; Vol. 2.

(7) Heck, R. F. *Org. React.* **1982**, *27*, 345–6. Examples of Heck coupling reaction utilized in polymer synthesis: (a) Greiner, A.; Heitz, W. *Polym. Prepr. (Am. Chem. Soc., Div. Polym. Chem.)* **1991**, *32*, 333. Heitz, W.; Brugging, W.; Freund, L.; Gailberger, M.; Greiner, A.; Jung, H.; Kampschulte, U.; Niebner, N.; Osan, F. *Makromol. Chem.* **1988**, *189*, 119. Martelock, H.; Greiner, A.; Heitz, W. *Makromol. Chem.* **1991**, *192*, 967. (b) Suzuki, M.; Lim, J. C.; Saegusa, T. *Macromolecules* **1990**, *23*, 1574. (c) Weitzel, H. P.; Mullen, K. *Makromol. Chem.* **1990**, *191*, 2837. (d) Boa, Z.; Chen, Y.; Cai, R.; Yu, L. *Macromolecules* **1993**, *26*, 5281.

(8) Strey, B. T. *J. Polym. Sci. Polym. Lett. Ed.* **1965**, 265.

(9) Henley, R. V.; Turner, E. E. *J. Chem. Soc.* **1930**, 939.

(10) Robello, D. R.; Dao, P. T.; Phelan, J.; Revelli, J.; Schildkraut, J. S.; Scozzafava, M.; Ulman, A.; Willand, C. S. *Chem. Mater.* **1992**, *4*, 425.

(11) Li, L.; Lee, J. Y.; Yang, Y.; Kumar, J.; Tripathy, S. K. *Appl. Phys. B* **1991**, *53*, 279.

(12) Teng, C. C.; Man, H. T. *Appl. Phys. Lett.* **1990**, *56*, 1734.

(13) Mitsunobu, O. *Synthesis* **1981**, 1.

MA950625V